Carbohydrate Polymers 114 (2014) 399–406

Contents lists available at ScienceDirect

Carbohydrate Polymers

journal homepage: www.elsevier.com/locate/carbpol

Collagen–poly(dialdehyde) guar gum based porous 3D scaffolds immobilized with growth factor for tissue engineering applications

Murali Ragothaman, Thanikaivelan Palanisamy*, Cheirmadurai Kalirajan

Advanced Materials Laboratory, Centre for Leather Apparel & Accessories Development, Central Leather Research Institute (Council of Scientific and Industrial Research), Adyar, Chennai 600020, India

ARTICLE INFO

Article history:
Received 21 May 2014
Received in revised form 8 July 2014
Accepted 11 August 2014
Available online 27 August 2014

Keywords:
Platelet-derived growth factor
Collagen
Poly(dialdehyde) guar gum
Cellularization
Porosity

ABSTRACT

Here we report the preparation of collagen–poly(dialdehyde) guar gum based hybrid functionalized scaffolds covalently immobilized with platelet derived growth factor – BB for tissue engineering applications. Poly(dialdehyde) guar gum was synthesized from selective oxidation of guar gum using sodium periodate. The synthesized poly(dialdehyde) guar gum not only promotes crosslinking of collagen but also immobilizes the platelet derived growth factor through imine bonds. The covalent crosslinking formed in collagen improves thermal, swelling and biodegradation properties of the hybrid scaffolds. The prepared hybrid scaffolds show 3D interconnected honeycomb porous structure when viewed under a microscope. The release of immobilized platelet derived growth factor was seen up to 13th day of incubation thereby proving its sustained delivery. The developed hybrid scaffold leads to a quantum increase in NIH 3T3 fibroblast cell density and proliferation thereby demonstrating its potential for tissue engineering applications.

1. Introduction

Tissue engineering is an attractive choice for treating damaged tissue/organs. Its applications has been shown to be successful in clinical treatment of regeneration of skin tissues (Metcalfe & Ferguson, 2007), nonvascularized tissues (Clarke, Lust, Sun, Black, & Ollerenshaw, 2001) and bone defects (Fukui, Sato, Kuboki, & Aoki, 2008). However, the stimulation of both cellularization and vascularization by tissue engineering construct has long been the quest in its application. The inadequate diffusion of nutrients in scaffolds also leads to reduced cell proliferation and survival (Patel & Mikos, 2004; Rivron, Liu, Rouwkema, de Boer, & van Blitterswijk, 2008). Hence, the synthesis of scaffolds with the specific bioactive stimulating factor coupled with porosity and biocompatibility has been the new focus of research. Collagen (C) has been widely used in tissue engineering due to the fact that it is the building block of skin and other tissues. Its distinct fibrous structure and biological functions such as low antigenicity and excellent biocompatibility makes it suitable for tissue engineering applications. However, the fast biodegradation rate and low mechanical strength of the native collagen necessitates stabilization or crosslinking, which is generally achieved using synthetic polymers or crosslinking agents such as glutaraldehyde (Murali, Anumary, Ashokkumar, Thanikaivelan, & Chandrasekaran, 2011). The use of these toxic chemicals is shown to exacerbate through depolymerisation and monomer release from the implants (Golomb et al., 1987; van Luyn et al., 1992). This led to the search for novel biocompatible and crosslinkable polymer for stabilizing collagen for the transient existence of the material.

Guar gum (GG) is one of the water-soluble, non-ionic, high-molecular weight plant polysaccharides derived from the endosperm of guar beans. It has been widely used in the pharmaceutical products primarily due to its high biocompatibility, biodegradability and rheological properties (Gliko-Kabir, Yagen, Baluom, & Rubinstein, 2000; Narasimha Murthy, Hiremath, & Paranjothy, 2004). Several studies have been carried out to increase the mechanical, thermal and viscosity properties of the GG by chemical modification (Huang, Lu, & Xiao, 2007; Huang, Yu, & Xiao, 2007). An approach has also been made to prepare poly(dialdehyde) guar gum (PDAGG) from GG using sodium periodate oxidation method (Wu et al., 2010). The periodate oxidation leads to cleavage of diol groups resulting in the formation of dialdehyde groups in the monosaccharide units of polysaccharide backbones thereby helping in immobilization of a drug by the formation of imine bonds (Takei, Sato, Ijima, & Kawakami, 2010). However, such modified GG has not yet been utilized for the preparation of hybrid scaffolds in conjunction with biopolymers such as collagen.

* Corresponding author. Tel.: +91 44 24910953; fax: +91 44 24910953.
E-mail addresses: thanik8@yahoo.com, thanik8@gmail.com (T. Palanisamy).

http://dx.doi.org/10.1016/j.carbpol.2014.08.045
0144-8617/

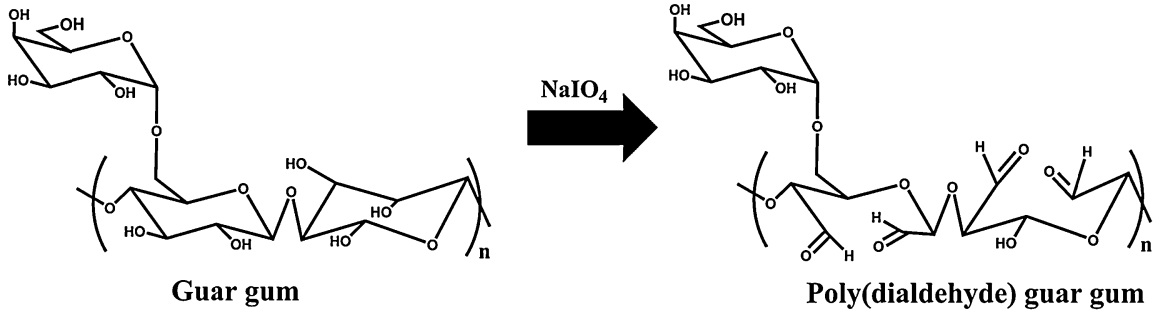

Fig. 1. Schematic showing the synthesis of PDAGG from GG.

The immobilization of bioactive factors in the scaffolds provides sustained drug release and transmit signals to activate the cell migration, differentiation and proliferation thereby leading to the formation of blood vessels and tissue regeneration (Chen & Mooney, 2003). Platelet derived growth factor – BB (PDGF) is one of the pleiotropic growth factor that promotes cell proliferation, chemotaxis and angiogenic response in vivo (Heldin & Westermark, 1999; Heldin, Östman, & Rönnstrand, 1998; Seppä, Grotendorst, Seppä, Schiffmann, & Martin, 1982). It stimulates pericyte production of extracellular matrix proteins such as fibronectin, collagen and proteoglycans, which are necessary for the basement membrane of capillaries and wound healing (Saik, Gould, Watkins, Dickinson, & West, 2011). The direct administration of PDGF and TGF-α in the genetically diabetic mouse has been shown to improve wound healing (Brown, Breeden, & Greenhalgh, 1994). Studies also reveal that the PDGF helps to breakdown old collagen by up-regulating matrix metalloproteinases (Jinnin et al., 2005).

Here, we synthesized PDAGG for stabilizing collagen and immobilizing PDGF in order to prepare hybrid scaffolds without employing toxic crosslinking agents. The prepared hybrid scaffolds were investigated for the crosslinking efficiency, structural morphology, biological properties, PDGF release and in vitro cell culture studies.

2. Materials and methods

2.1. Materials

The raw cowhide trimmed wastes were collected from pilot tannery at Central Leather Research Institute (CLRI), Chennai. Guar gum, potassium iodine (KI), ethylene glycol, Dulbecco's modified Eagle's medium (DMEM), fetal bovine serum (FBS) and the supplementary antibiotics for tissue culture were purchased from Himedia, India. Sodium periodate and sodium bicarbonate were purchased from M/s Sisco Research Lab, Mumbai, India. Starch was procured from M/s SD Fine-Chem, Mumbai, India. 2,4,6-trinitrobenzene sulfonic acid (TNBS, 5% w/v in H_2O), protease from *Aspergillus saitoi* and 3-(4,5-dimethylthiazol-2-yl)-2,5-diphenyltetrazolium bromide (MTT) were purchased from Sigma-Aldrich, India. The mouse NIH 3T3 fibroblast cells were obtained from the National Centre for Cell Science (NCCS), Pune, India. Human recombinant platelet-derived growth factor-BB (PDGF-BB, CYT-501) was purchased from Prospec Bio, Isreal. PDGF-BB Standard ELISA development kit was procured from Peprotech Ltd. All other reagents were of high analytical grade.

2.2. Preparation of collagen solution

Hide powder from the raw cowhide trimmings was prepared according to our previously reported procedure (Ashokkumar et al., 2012; Murali et al., 2011). Briefly, the collected raw hide trimming pieces were soaked, limed, dehaired, relimed, fleshed and delimed using the conventional procedures (Saravanabhavan, Aravindhan, Thanikaivelan, Rao, & Nair, 2003; Thanikaivelan, Rao, Nair, & Ramasami, 2002) to remove unwanted keratin, elastin, reticulin, albumin, globulin, proteoglycan and fats. The delimed hide pieces were soaked in 35% and 70% acetone, followed by 100% methanol for sufficient duration. Finally, the hide pieces were thoroughly dried in a vacuum drier and made into fine powder using a Willy mill of mesh size 2 mm. About 2 g of hide powder was weighed and dissolved in 100 ml of 0.5 N glacial acetic acid at 4 °C for 2 h. After the complete solubilisation, the collagen solution was stored in the amber bottle under the refrigerated condition. The composition of collagen in the hide powder was analyzed by estimating the hydroxyproline content using standard procedure (Woessner, 1961) and found to be 90 ± 1.8%.

2.3. Synthesis of poly(dialdehyde) guar gum

PDAGG was synthesized by oxidizing the —OH group to —CHO group in the monosaccharide units of GG using sodium periodate based oxidation method (Gomez, Rinaudo, & Villar, 2007) as shown in Fig. 1. About 1 g of GG was dissolved in 200 ml distilled water and stirred to get homogenous solution for 30 min. To this solution, 1.5 g of sodium periodate dissolved in 25 ml distilled water was added and kept for stirring in dark at 35 °C for 24 h. Then, 1 ml of ethylene glycol was added and stirred for 1 h to quench the reaction by inactivating the unreacted periodate. The reaction solution was centrifuged to collect the supernatant at 10,000 rpm for 10 min. Then, the supernatant solution was treated with 900 ml acetone (1:4 ratio) to precipitate the synthesized PDAGG polymer. The collected PDAGG precipitate was washed with acetone three times. Finally, the precipitated PDAGG was lyophilized and then powdered. The amount of synthesized PDAGG polymer was 0.6 g (60% yield).

2.4. Degree of oxidation

The degree of oxidation or aldehyde formation was determined by measuring the percentage of periodate consumption using KI–Thyodene indicator method (Gomez et al., 2007). The indicator solution was freshly prepared by mixing equal volumes of KI (20% w/v in pH 7.0 phosphate buffer) and thyodene solution (starch 1% w/v in pH 7.0 phosphate buffer). Samples were drawn at different time intervals such as 0, 0.25, 0.5, 0.75, 1, 2, 4, 8, 12 and 24 h during the oxidation process (as given in Section 2.3). One millilitre of sample was diluted to 250 ml using distilled water. Then, 3 ml of diluted sample was mixed with 1.5 ml indicator solution. The blank solution was comprised of 3 ml distilled water and 1.5 ml indicator solution. Finally, the total volume was made up to 5 ml by adding distilled water. The absorbance of triiodine–starch complex was measured using a UV–Visible spectrophotometer (UV-1800, Shimadzu) at 486 nm. The difference between initial and final value of absorbance corresponds to periodate consumption and degree of

oxidation in the reaction. The degree of oxidation (or aldehyde formation) and periodate residual was calculated using the Eqs. (1) and (2) as below.

$$\text{Degree of oxidation}(\%) = \frac{\text{Initial absorbance}_{\text{value}} - \text{Final absorbance}_{\text{value}}}{\text{Initial absorbance}_{\text{value}}} \times 100 \quad (1)$$

$$\text{Periodate residual}(\%) = 100 - \left[\frac{\text{Initial absorbance}_{\text{value}} - \text{Final absorbance}_{\text{value}}}{\text{Initial absorbance}_{\text{value}}} \times 100\right] \quad (2)$$

2.5. Preparation of hybrid scaffolds

1.5 g of PDAGG was dissolved in 50 ml distilled water by continuous stirring at 80 °C for 2 h. Then, 10 ml of collagen solution was taken in a clean vial and stirred with different concentrations of PDAGG from 25 to 100 wt% for 30 min at room temperature to induce crosslinking between the amino group of collagen and aldehyde group of PDAGG through Schiff's base reaction. The formed viscous solutions were transferred into the Petri plates ($200 \times 25\ mm^2$ dimension) and freeze dried to obtain hybrid scaffolds with combinations such as 100/0, 100/25, 100/50, 100/75 and 100/100 wt% C/PDAGG, as shown in Fig. S1. The prepared scaffolds were stored under the refrigerated condition.

2.6. Characterization of hybrid scaffolds

2.6.1. FTIR analysis

The collagen, GG, PDAGG and hybrid scaffolds were analyzed using Perkin Elmer FT-IR spectrometer. The samples were ground with KBr and compressed to form pellets. The pellets were analyzed in a single beam mode at the range of 400–4000 cm^{-1} with an average of four scans and 2 cm^{-1} resolution.

2.6.2. Determination of crosslinking efficiency

The crosslinking efficiency of PDAGG with collagen was determined using TNBS assay (Jayakumar et al., 2012). Briefly, 0.5 ml of sample (before lyophilisation step) was added to 1 ml of 4% w/v $NaHCO_3$ and 1 ml of freshly prepared 0.5% (v/v) TNBS solution in distilled water. The solution was vortex mixed and kept at 60 °C for 4 h. After that, 1 ml of solution was transferred to fresh test tube and 3 ml of 6 M HCl was added. The tubes were kept at 40 °C for 1.5 h and the maximum absorbance of formed trinitrophenyl complex was measured using UV–Visible spectrophotometer (UV-1800, Schimadzu) at 420 nm. The native collagen solution was also treated with TNBS in a similar manner as a control. The crosslinking efficiency and free amino group was determined using the Eqs. (3) and (4) as below.

$$\text{Crosslinking efficiency}(\%) = \frac{\text{Control absorbance}_{\text{value}} - \text{Sample absorbance}_{\text{value}}}{\text{Control absorbance}_{\text{value}}} \times 100 \quad (3)$$

$$\text{Free amino group}(\%) = 100 - \left[\frac{\text{Control absorbance}_{\text{value}} - \text{Sample absorbance}_{\text{value}}}{\text{Control absorbance}_{\text{value}}} \times 100\right] \quad (4)$$

2.6.3. Differential scanning calorimetric analysis

The hydrothermal stability of select hybrid wet scaffolds 100/0 and 100/100 wt% C/PDAGG was measured using differential scanning calorimeter (DSC Q200, TA Instrument). About 5 mg of wet samples were loaded in aluminium pans and heated at the rate of 1 °C/min from 30 to 100 °C in nitrogen flow of 50 ml/min.

2.6.4. Scanning electron microscopic analysis

The surface morphology of select hybrid scaffolds 100/0 and 100/100 wt% C/PDAGG was analyzed using scanning electron microscope (SEM, Tescan Vega 3 SB) at an accelerating voltage of 3 kV in different magnifications. The samples were cut and mounted on aluminium stubs and coated with gold using Tescan sputter coater before the analysis.

2.6.5. Swelling studies

The in vitro swelling behavior of hybrid scaffolds was assessed by soaking a known weight of scaffolds in 25 ml of 0.05 M phosphate buffered saline (PBS) solution (pH 7.4). The swollen weight of scaffolds was measured at 0.25, 0.5, 1, 2, 4, 6, 8, 10 and 12 h after removing the surface moisture using filter paper. The extent of swelling of hybrid scaffolds was calculated using the Eq. (5) as below.

$$\text{Swelling}(\%) = \frac{\text{Swellen weight} - \text{Initial weight}}{\text{Initial weight}} \times 100 \quad (5)$$

2.6.6. In vitro biodegradation studies

The in vitro biodegradation of scaffolds was assessed by incubating a known weight of scaffolds in 25 ml PBS (pH 7.4) along with 10 mg of protease at 37 °C for 24 h. After the completion of incubation time, the samples were centrifuged at 10,000 rpm for 10 min, freeze dried and then weighed. This process was repeated for four times (with 24 h interval) using fresh protease solution. The extent of in vitro biodegradation of hybrid scaffolds was calculated using the Eq. (6) as below.

$$\text{In vitro biodegradation}(\%) = \frac{\text{Initial weight} - \text{Biodegraded weight}}{\text{Initial weight}} \times 100 \quad (6)$$

2.7. Covalent immobilization of PDGF in hybrid scaffolds

Five millilitre of collagen solution was blended with 100 wt% PDAGG and 1 ml of 1 μg/ml PDGF solution for 30 min for covalent immobilization of PDGF as shown in Fig. 2. The blended solution was transferred into the Petri plates ($110 \times 25\ mm^2$ dimension) and freeze dried to obtain 100/100 wt% C/PDAGG loaded with 1 μg PDGF hybrid scaffolds. The prepared hybrid scaffolds were stored under the refrigerated condition.

2.8. In vitro PDGF release studies

The in vitro PDGF release was determined using the enzyme-linked immunosorbent assay (ELISA). Briefly, the prepared 100/100 wt% C/PDAGG loaded with 1 μg PDGF hybrid scaffold was incubated in 10 ml of PBS solution (pH 7.4) at 37 °C. At regular intervals, 100 μl of the medium was replaced by fresh PBS for measuring the concentration of growth factor. The released PDGF from the hybrid scaffolds was determined by ELISA technique using microplate reader (Epoch, BioTek) at 405 nm with wavelength correction set

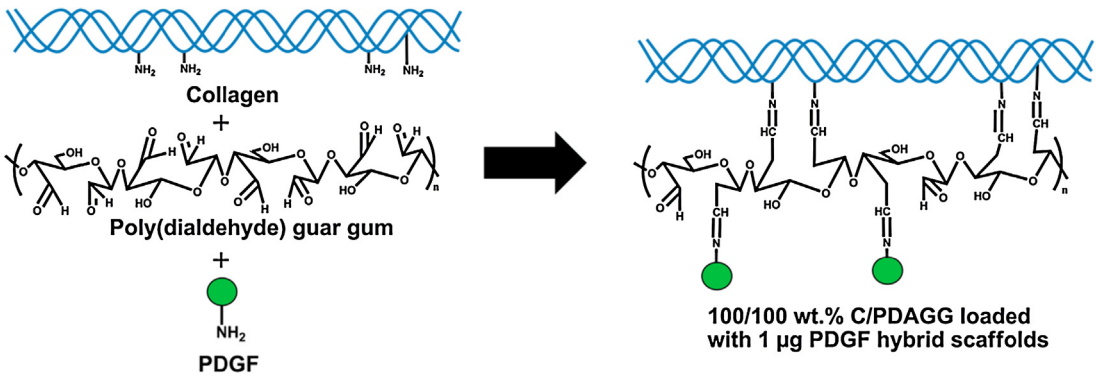

Fig. 2. Schematic showing the covalent immobilization of PDGF in 100/100 wt% C/PDAGG hybrid scaffolds.

at 650 nm. The in vitro PDGF release was calculated using the Eq. (7) given below.

$$\text{In vitro PDGF release}(\%) = \frac{\text{Amount of PDGF released}}{\text{Initial amount of PDGF}} \times 100 \quad (7)$$

2.9. In vitro cell culture studies

The viability and proliferation of NIH 3T3 fibroblast cells were studied for select hybrid scaffolds such as 100/0, 100/100 wt% C/PDAGG and 100/100 wt% C/PDAGG loaded with 1 μg PDGF. The circular samples with a diameter of 1 cm were sterilized with culture plates by ethylene oxide (EtO) method. To this, 300 μl of NIH 3T3 fibroblast cell suspension (2×10^6 cells/ml) was slowly dispersed over the surface of sterilized samples placed in a 24-well culture plate and maintained in DMEM with 10% FBS supplemented with penicillin (100 units/ml), streptomycin (100 μg/ml) and amphotericin B (0.25 μg/ml) at 37 °C, humidified with 5% CO_2. The cells cultured in a blank well were used as a control. Seeded cells were cultured for 48 h and the medium was changed every day. The number of viable cells in the select hybrid scaffold combinations was determined using MTT assay at 570 nm. The cell morphology of 100/100 wt% C/PDAGG loaded with 1 μg PDGF hybrid scaffolds was investigated using scanning electron microscopy. The 100/100 wt% C/PDAGG loaded with 1 μg PDGF hybrid scaffolds were rinsed with PBS after 48 h of cell seeding and fixed using 10% neutral formalin buffer for 5 h at 4 °C and dehydrated by lyophilisation before SEM analysis.

3. Results and discussion

3.1. Synthesis and characterization of PDAGG

The periodate oxidation of GG leads to the cleavage of diol groups in the monosaccharide units of GG, resulting in the formation of aldehyde groups in the polymeric backbones (Wu et al., 2010). The degree of oxidation and the extent of periodate residual in GG during the course of reaction are shown in Fig. 3a. It is seen that the degree of oxidation (or formation of aldehyde) is up to 98% at 24th hour of reaction. After the completion of reaction, the periodate residual is 2% in the reaction solution. It is also seen that 50% of GG is oxidized to PDAGG within the 1st hour of reaction after which the reaction attained a steady state. These results indicate that the sodium periodate based oxidation leads to the formation of aldehyde groups in GG thereby forms PDAGG (Gomez et al., 2007; Wu et al., 2010).

FTIR spectra of pure GG and PDAGG are shown in Fig. 3b. The FTIR spectrum of pure GG exhibits a broad characteristic peak at 3198 cm^{-1} corresponding to the presence of significant quantity of —OH group arising from polysaccharide units. After the periodate oxidation process, the modified GG shows characteristic bands at 1738, 1028 and 770 cm^{-1}. The formation of —CHO group in place of —OH group in GG is evident from the appearance of a low intense C=O stretching band at 1738 cm^{-1}. The observed low intensity in spite of 98% oxidation may be due to the formation of hemiacetal

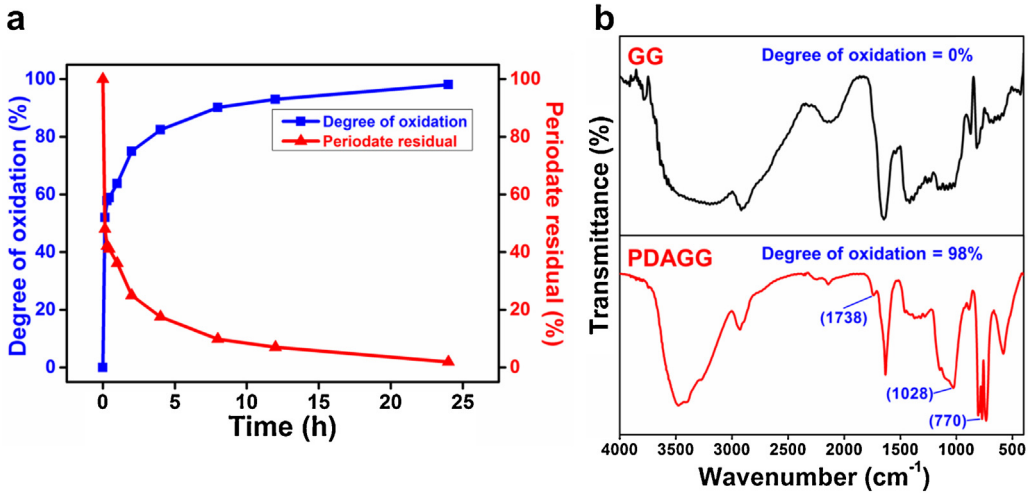

Fig. 3. (a) Degree of oxidation and periodate residual during the modification of GG using sodium periodate method; (b) FTIR spectra of pure GG and PDAGG.

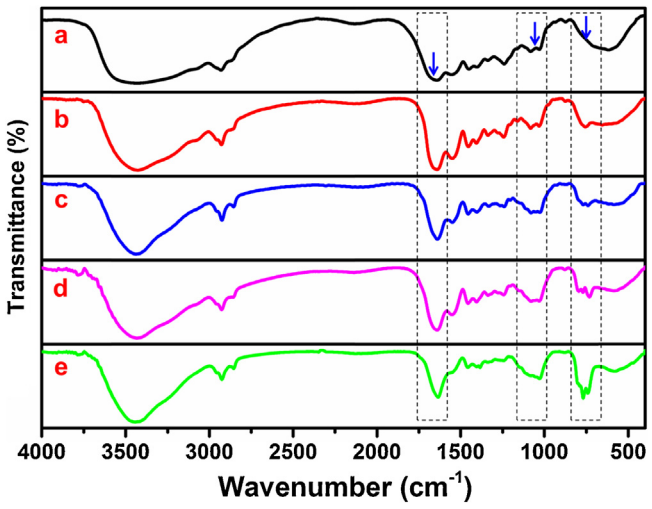

Fig. 4. FTIR spectra of (a) pure collagen scaffold, (b) 100/25, (c) 100/50, (d) 100/75 and (e) 100/100 wt% C/PDAGG hybrid scaffolds.

and/or hydrated bonds between the aldehyde and hydroxyl groups (Kim, Kuga, Wada, Okano, & Kondo, 2000; Wu et al., 2010). Further, the PDAGG shows more sharper and intense peaks around 1028 and 770 cm^{-1} due to the C—O—C stretching and C—H out of plane bending arising from the formation of hemiacetal and hydration of aldehydes (Kim et al., 2000; Wu et al., 2010). It is also seen that broad peak corresponding to —OH group is shifted from 3198 cm^{-1} to a sharp peak at 3479 cm^{-1} probably due to the hydration of —CHO groups in GG. Although the aldehyde functionality can convert into hemiacetal or as hydrates, it should be noted that these reactions are unstable and reversible. Hence, these results confirm the formation of aldehyde groups in GG.

3.2. Crosslinking of collagen with PDAGG

FTIR spectra of pure collagen and C/PDAGG hybrid scaffolds are shown in Fig. 4. FTIR spectrum of collagen depicts the characteristic peaks at 1642, 1554 and 1240 cm^{-1}, which corresponds to amide I, amide II and amide III groups, respectively (Fig. 4a). FTIR spectra of prepared hybrid scaffolds did not show the characteristic peaks of PDAGG (Fig. 4b–e), which may be due to the crosslinking between the aldehyde groups of PDAGG with the amine groups of collagen resulting in the formation of imine bond. The characteristic peak of imine bond associated with the C=N linkage is generally shown as a strong stretching absorption around 1620 cm^{-1} (Hua, Chen, Tsai, Lin, & Wang, 2011; Meyer, Joiner, & Stoddart, 2007). However, in this study, collagen also exhibits a less-sharp peak at 1642 cm^{-1} due to the amide I group. Nonetheless, the peak at 1620 cm^{-1} has become more sharpened and concerted as the concentration of PDAGG increases in the C/PDAGG hybrid scaffolds as shown by the arrows in Fig. 4. Further, it is also seen that the peaks corresponding to anhydroglucose rings around 1028 and 770 cm^{-1} also became sharper and intense as the concentration of PDAGG increased in the hybrid scaffolds. Magnified FTIR spectra of the hybrid scaffolds are given in Fig. S2 for better comparison and visualization. These results provide convincing evidence for the formation of imine bond between collagen and PDAGG resulting in homogenous hybrid scaffolds.

PDAGG crosslinks collagen by the formation of stable covalent imine bonding between the amino groups of lysine, hydroxylysine and arginine from collagen and aldehyde group of PDAGG through the Schiff's base reaction (Jayakumar et al., 2012). The crosslinking efficiency of PDAGG with collagen was found by estimating the unreacted/excess amino group of collagen. It is well known that the TNBS reacts with amines, hydrazines and hydrazides groups to form a stable trinitrophenyl complex. The excess amount of amino group in collagen molecule reacts with the TNBS to form stable trinitrophenyl complex and determined using UV-Visible spectrophotometer. Fig. 5a shows the crosslinking efficiency of PDAGG with collagen in the prepared hybrid scaffolds. It is seen that the crosslinking increases as the concentration of PDAGG increases and attains a maximum of 75% for the 100/100 wt% C/PDAGG hybrid scaffolds. In other words, 100/100 wt% C/PDAGG hybrid scaffolds possess about only 25% free amino groups. The plant biopolymer crosslinked collagen is stable, as later verified by DSC analysis, and completely avoids toxic crosslinking agents such as glutaraldehyde (Jayakumar et al., 2012).

The wet pristine collagen and 100/100 wt% C/PDAGG hybrid scaffolds were analyzed using DSC to understand their hydrothermal stability. Fig. 5b shows that the shrinkage temperature of wet pristine collagen scaffolds is around 58 °C. Whereas the 100/100 wt% C/PDAGG hybrid scaffolds exhibit a shrinkage temperature of 71 °C. It is seen that the hydrothermal stability of the pristine collagen is increased by the addition of PDAGG, which is due to the crosslinking between the amino functional groups of collagen and aldehyde groups of PDAGG (Jayakumar et al., 2012). These results are in agreement with the results obtained from FTIR analysis and crosslinking efficiency of PDAGG.

3.3. Morphology of hybrid scaffolds

Surface morphology of 100/0 and 100/100 wt% C/PDAGG hybrid scaffolds was analyzed using SEM as shown in Fig. 6. The surface of un-crosslinked 100/0 wt% C/PDAGG scaffold seems to be

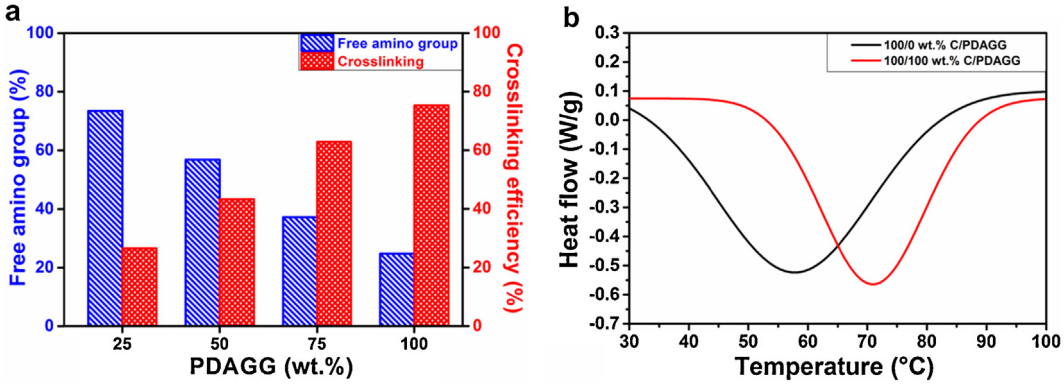

Fig. 5. (a) Crosslinking efficiency of PDAGG with collagen and free amino group in collagen with varying amount of PDAGG; (b) DSC traces showing the hydrothermal stability of wet pristine collagen and 100/100 wt% C/PDAGG hybrid scaffolds.

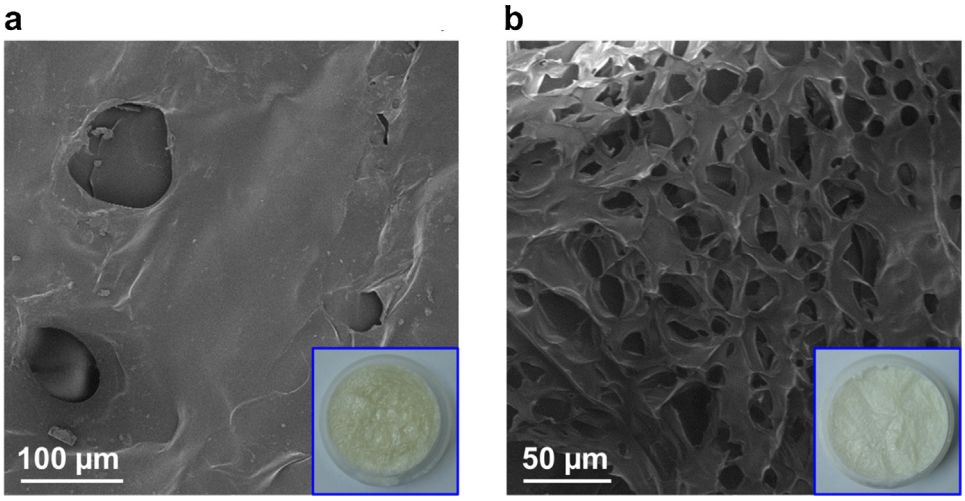

Fig. 6. Scanning electron microscopic images showing the morphology of (a) 100/0 and (b) 100/100 wt% C/PDAGG hybrid scaffolds. Insets show digital images of respective as-prepared freeze dried scaffolds.

smooth with less porous (Fig. 6a). Whereas the crosslinked 100/100 wt% C/PDAGG hybrid scaffold exhibits smooth surface with numerous pores over several layers (Fig. 6b). Additional SEM images are shown in Fig. S3. This layered porous architecture provides a 3D honeycomb like structure in the prepared hybrid scaffolds with an average pore size of 15 ± 7 μm (Fig. S4). These results indicate that the difference in morphology is mainly due to the crosslinking of collagen with PDAGG molecules. The increased porosity in the prepared hybrid scaffolds is expected to promote cell adhesion, drug release and cellularization (Zhao et al., 2011).

3.4. *In vitro swelling and biodegradation properties of PDAGG stabilized collagen scaffolds*

Fig. 7a shows the in vitro swelling behavior of pure collagen and C/PDAGG hybrid scaffolds. It is seen that the pure collagen scaffolds attain a maximum swelling around 1500% after 12 h incubation. Whereas the C/PDAGG hybrid scaffolds exhibit significantly reduced swelling up to 580%. It is interesting to note that the extent of swelling reduces as the concentration of PDAGG increases in the hybrid scaffolds. It also illustrates that the pure collagen reaches equilibrium stage after 8 h, whereas the developed hybrid scaffolds attains within 1 h of incubation. This could be due to the increased porosity in the prepared hybrid scaffolds, which can facilitate the cell to penetrate inside the scaffold and grow in a three dimensional fashion.

The in vitro biodegradation rate directly demonstrates the biostability of hybrid scaffolds in biological fluids during tissue engineering application. The in vitro biodegradation patterns of pure collagen and different C/PDAGG hybrid scaffolds are shown in Fig. 7b. As can be seen, the un-crosslinked collagen scaffold quickly biodegraded up to 43% at the 1st day of incubation. After which, the biodegradation gradually increased and the scaffold completely dissolved after 5th day of incubation. Whereas the crosslinked C/PDAGG hybrid scaffolds demonstrate reduced biodegradation rate as a function of concentration of PDAGG in collagen. Lowest biodegradation of 21% was observed for 100/100 wt% C/PDAGG hybrid scaffold after 5th day of incubation. The observed stability against biodegradation appears to be much higher compared to the collagen physically blended with starch and soy protein (Murali et al., 2011). These results reveal that the prepared hybrid scaffolds possess improved biostability due to the crosslinking between collagen and PDAGG molecules.

3.5. *PDGF-BB promotes cellularization in hybrid scaffolds*

The drug (PDGF) release profile from 100/100 wt% C/PDAGG loaded with 1 μg PDGF hybrid scaffolds was investigated and the results are shown in Fig. 8a. It is seen that the PDGF is released rapidly at the beginning and then gradually reduced during the course of incubation. The initial rapid release of PDGF may be due to the quick biodegradation tendency of C/PDAGG hybrid scaffold at the initial period of incubation. Therefore, the sustained PDGF release, up to 13th day of incubation, may be due to the interaction between the amine group of PDGF and aldehyde group of PDAGG to form imine bonds (Maia et al., 2012). As the 100/100 wt% C/PDAGG

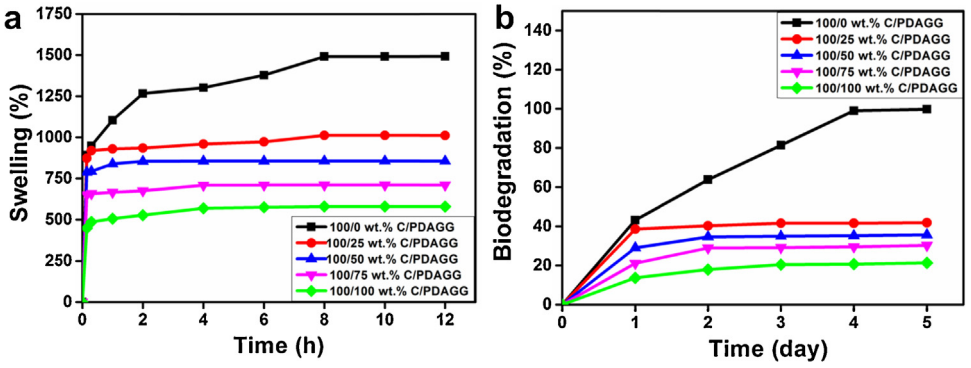

Fig. 7. (a) In vitro swelling and (b) in vitro biodegradation patterns of 100/0, 100/25, 100/50, 100/75 and 100/100 wt% C/PDAGG hybrid scaffolds.

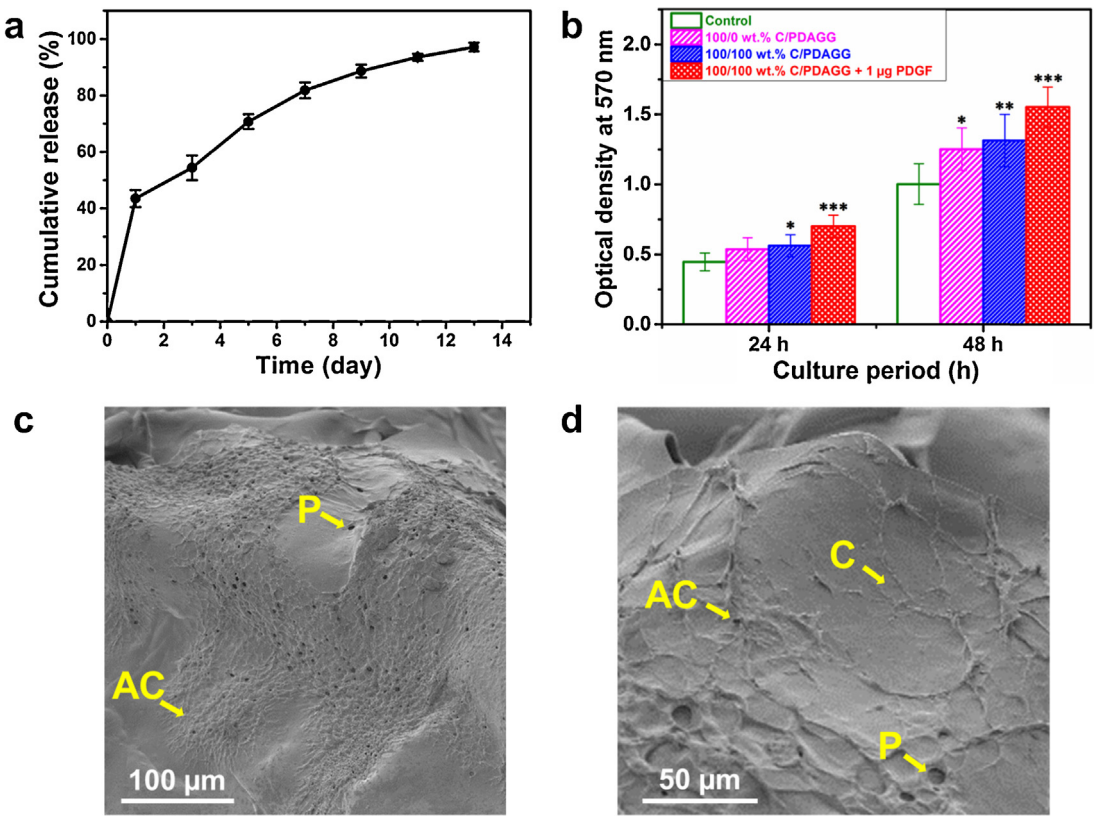

Fig. 8. (a) In vitro drug release pattern of covalently immobilized 100/100 wt% C/PDAGG loaded with 1 μg PDGF hybrid scaffolds; (b) In vitro NIH 3T3 fibroblast cell proliferation patterns of control (blank polystyrene well plate), 100/0, 100/100 wt% C/PDAGG and 100/100 wt% C/PDAGG loaded with 1 μg PDGF hybrid scaffolds. Values are expressed as mean ± SD for six samples and the results were statistically evaluated using students *t* test. The level of significance is expressed as * $p \leq 0.05$, ** $p \leq 0.01$ and *** $p \leq 0.001$, respectively, compared with the corresponding controls; (c) and (d) Scanning electron microscopic images showing the surface of 48 h cell cultured 100/100 wt% C/PDAGG loaded with 1 μg PDGF hybrid scaffolds at lower and higher magnification, respectively. AC, C and P refer to aggregated cells, individual cells and small pores, respectively. Images show significant quantity of NIH 3T3 fibroblast cell proliferation, both AC and C, on the surface due to the release of PDGF.

loaded with 1 μg PDGF hybrid scaffolds undergo biodegradation, the PDGF–PDAGG imine bond may break leading to the release of PDGF.

The in vitro NIH 3T3 fibroblast cell viability and proliferation studies in control (blank polystyrene well plate), 100/0, 100/100 wt% C/PDAGG and 100/100 wt% C/PDAGG loaded with 1 μg PDGF hybrid scaffolds were carried out using MTT assay and the results are shown in Fig. 8b. The fibroblast cell proliferation data after 48 h shows a gradual increase in the number of cells up to 25% and 31% for the 100/0 and 100/100 wt% C/PDAGG hybrid scaffolds as against the blank cultured cells. The slight increase in the cell proliferation for the 100/100 wt% C/PDAGG hybrid scaffold compared to the 100/0 wt% C/PDAGG scaffold may be due to the increased porosity in the hybrid scaffolds owing to the crosslinking between collagen and PDAGG. On the other hand, the 100/100 wt% C/PDAGG loaded with 1 μg PDGF hybrid scaffold exhibits maximum number of fibroblast cells (55% increment) compared to the control. This rapid proliferation may be due to the high porosity coupled with the release of PDGF from the hybrid scaffolds (Zhao et al., 2011).

Fig. 8c and d shows the morphology of NIH 3T3 fibroblasts cells cultured after 48 h in 100/100 wt% C/PDAGG loaded with 1 μg PDGF hybrid scaffolds at lower and higher magnification, respectively. The electron microscopic images show that more number of fibroblast cells is adhered on the surface of scaffolds. It is interesting to note that the honeycomb porous structure of scaffolds is not seen in the images, which is due to the adherence of more number of fibroblast cells on the pore walls of the scaffolds and further formation of interconnections between the cells. The presence of aggregated cells (AC) and small pores (P) are marked in the images (Fig. 8c). Higher magnification image of the scaffold shows the presence of individual cells (C) along with AC and small pores (Fig. 8d). The results corroborate the fact that the highly proliferated fibroblast cells in the scaffolds are due to the increased porosity and platelet derived growth factors. In general, PDGF is one of the most important chemoattractants and mitogens for fibroblasts, glial cells and smooth muscle cells (Seppä et al., 1982). It is a required element for the fibroblast cells to stimulate the chemotaxis, proliferation and gene expression in the cells (Sasaki et al., 2000; Tingstrom, Heldin, & Rubin, 1992). Hence, the results demonstrate that the inclusion of PDGF in the hybrid scaffolds provides good biocompatibility and cellularization. Therefore, the prepared hybrid scaffolds can be used to accelerate extracellular collagen matrix formation and to promote vascularization thereby forms as an ideal candidate for tissue engineering application.

4. Conclusions

PDAGG crosslinked collagen based hybrid scaffolds covalently immobilized with PDGF were prepared for tissue engineering applications. FTIR, crosslinking efficiency and DSC studies reveal that the PDAGG stabilized the collagen and immobilized PDGF in the C/PDAGG scaffolds due to the formation of imine bonds. The prepared hybrid scaffolds have better thermal, swelling and biodegradation properties. Crosslinking of collagen using PDAGG leads to interconnected 3D porous structure as seen in SEM. The in vitro release of immobilized PDGF-BB is seen up to 13th day of incubation demonstrating the sustained delivery over long period. We have also demonstrated excellent growth and proliferation of NIH 3T3 fibroblast cells seeded on the surface of PDGF immobilized hybrid scaffolds owing to their porous structure and release of

PDGF. Hence, the results suggest that the stabilized and functionalized C/PDAGG hybrid scaffolds loaded with PDGF provide good cellularization thereby promising as an effective system for tissue engineering applications.

Acknowledgments

Authors thank SERC, Department of Science and Technology, India for providing financial assistance under the Fast Track Scheme for Young Scientists (SERC/ET-0359/2011). CSIR-CLRI Communication No. 1066.

Appendix A. Supplementary data

Supplementary data associated with this article can be found, in the online version, at http://dx.doi.org/10.1016/j.carbpol.2014.08.045.

References

Ashokkumar, M., Sumukh, K. M., Murali, R., Narayanan, N. T., Ajayan, P. M., & Thanikaivelan, P. (2012). Collagen-chitosan biocomposites produced using nanocarbons derived from goatskin waste. *Carbon*, *50*, 5574–5582.

Brown, R. L., Breeden, M. P., & Greenhalgh, D. G. (1994). PDGF and TGF-α act synergistically to improve wound healing in the genetically diabetic mouse. *Journal of Surgical Research*, *56*, 562–570.

Chen, R. R., & Mooney, D. J. (2003). Polymeric growth factor delivery strategies for tissue engineering. *Pharmaceutical Research*, *20*, 1103–1112.

Clarke, D. R., Lust, R. M., Sun, Y. S., Black, K. S., & Ollerenshaw, J. D. (2001). Transformation of nonvascular acellular tissue matrices into durable vascular conduits. *The Annals of Thoracic Surgery*, *71*, S433–S436.

Fukui, N., Sato, T., Kuboki, Y., & Aoki, H. (2008). Bone tissue reaction of nano-hydroxyapatite/collagen composite at the early stage of implantation. *Bio-Medical Materials and Engineering*, *18*, 25–33.

Gliko-Kabir, I., Yagen, B., Baluom, M., & Rubinstein, A. (2000). Phosphated crosslinked guar for colon-specific drug delivery. II. In vitro and in vivo evaluation in the rat. *Journal of Controlled Release*, *63*, 129–134.

Golomb, G., Schoen, F. J., Smith, M. S., Linden, J., Dixon, M., & Levy, R. J. (1987). The role of glutaraldehyde-induced cross-links in calcification of bovine pericardium used in cardiac-valve bioprostheses. *The American Journal of Pathology*, *127*, 122–130.

Gomez, C. G., Rinaudo, M., & Villar, M. A. (2007). Oxidation of sodium alginate and characterization of the oxidized derivatives. *Carbohydrate Polymers*, *67*, 296–304.

Heldin, C.-H., Östman, A., & Rönnstrand, L. (1998). Signal transduction via platelet-derived growth factor receptors. *Biochimica et Biophysica Acta (BBA)—Reviews on Cancer*, *1378*, F79–F113.

Heldin, C.-H., & Westermark, B. (1999). Mechanism of action and in vivo role of platelet-derived growth factor. *Physiological Reviews*, *79*, 1283–1316.

Hua, M. Y., Chen, H. C., Tsai, R. Y., Lin, Y. C., & Wang, L. (2011). A novel biosensing mechanism based on a poly(N-butyl benzimidazole)-modified gold electrode for the detection of hydrogen peroxide. *Analytica Chimica Acta*, *693*, 114–120.

Huang, Y., Lu, J., & Xiao, C. (2007). Thermal and mechanical properties of cationic guar gum/poly(acrylic acid) hydrogel membranes. *Polymer Degradation and Stability*, *92*, 1072–1081.

Huang, Y., Yu, H., & Xiao, C. (2007). pH-sensitive cationic guar gum/poly (acrylic acid) polyelectrolyte hydrogels: Swelling and in vitro drug release. *Carbohydrate Polymers*, *69*, 774–783.

Jayakumar, G. C., Kanth, S. V., Sai, K. P., Chandrasekaran, B., Rao, J. R., & Nair, B. U. (2012). Scleraldehyde as a stabilizing agent for collagen scaffold preparation. *Carbohydrate Polymers*, *87*, 1482–1489.

Jinnin, M., Ihn, H., Mimura, Y., Asano, Y., Yamane, K., & Tamaki, K. (2005). Regulation of fibrogenic/fibrolytic genes by platelet-derived growth factor C, a novel growth factor, in human dermal fibroblasts. *Journal of Cellular Physiology*, *202*, 510–517.

Kim, U.-J., Kuga, S., Wada, M., Okano, T., & Kondo, T. (2000). Periodate oxidation of crystalline cellulose. *Biomacromolecules*, *1*, 488–492.

Maia, J., Vazao, H., Pedroso, D. C., Jesus, C. S., Brito, R. M., Graos, M., et al. (2012). VEGF-functionalized dextran has longer intracellular bioactivity than VEGF in endothelial cells. *Biomacromolecules*, *13*, 2906–2916.

Metcalfe, A. D., & Ferguson, M. W. (2007). Bioengineering skin using mechanisms of regeneration and repair. *Biomaterials*, *28*, 5100–5113.

Meyer, C. D., Joiner, C. S., & Stoddart, J. F. (2007). Template-directed synthesis employing reversible imine bond formation. *Chemical Society Reviews*, *36*, 1705–1723.

Murali, R., Anumary, A., Ashokkumar, M., Thanikaivelan, P., & Chandrasekaran, B. (2011). Hybrid biodegradable films from collagenous wastes and natural polymers for biomedical applications. *Waste and Biomass Valorization*, *2*, 323–335.

Narasimha Murthy, S., Hiremath, S. R. R., & Paranjothy, K. (2004). Evaluation of carboxymethyl guar films for the formulation of transdermal therapeutic systems. *International Journal of Pharmaceutics*, *272*, 11–18.

Patel, Z. S., & Mikos, A. G. (2004). Angiogenesis with biomaterial-based drug- and cell-delivery systems. *Journal of Biomaterials Science, Polymer Edition*, *15*, 701–726.

Rivron, N. C., Liu, J., Rouwkema, J., de Boer, J., & van Blitterswijk, C. A. (2008). Engineering vascularised tissues in vitro. *European Cells and Materials*, *15*, 27–40.

Saik, J. E., Gould, D. J., Watkins, E. M., Dickinson, M. E., & West, J. L. (2011). Covalently immobilized platelet-derived growth factor-BB promotes angiogenesis in biomimetic poly(ethylene glycol) hydrogels. *Acta Biomaterialia*, *7*, 133–143.

Saravanabhavan, S., Aravindhan, R., Thanikaivelan, P., Rao, J. R., & Nair, B. U. (2003). Green solution for tannery pollution: Effect of enzyme based lime-free unhairing and fibre opening in combination with pickle-free chrome tanning. *Green Chemistry*, *5*, 707–714.

Sasaki, M., Kashima, M., Ito, T., Watanabe, A., Sano, M., Kagaya, M., et al. (2000). Effect of heparin and related glycosaminoglycan on PDGF-induced lung fibroblast proliferation, chemotactic response and matrix metalloproteinases activity. *Mediators of Inflammation*, *9*, 85–91.

Seppä, H., Grotendorst, G., Seppä, S., Schiffmann, E., & Martin, G. R. (1982). Platelet-derived growth factor in chemotactic for fibroblasts. *The Journal of Cell Biology*, *92*, 584–588.

Takei, T., Sato, M., Ijima, H., & Kawakami, K. (2010). In situ gellable oxidized citrus pectin for localized delivery of anticancer drugs and prevention of homotypic cancer cell aggregation. *Biomacromolecules*, *11*, 3525–3530.

Thanikaivelan, P., Rao, J. R., Nair, B. U., & Ramasami, T. (2002). Zero discharge tanning: A shift from chemical to biocatalytic leather processing. *Environmental Science and Technology*, *36*, 4187–4194.

Tingstrom, A., Heldin, C.-H., & Rubin, K. (1992). Regulation of fibroblast-mediated collagen gel contraction by platelet-derived growth factor, interleukin-1 alpha and transforming growth factor-beta 1. *Journal of Cell Science*, *102*, 315–322.

van Luyn, M. J., van Wachem, P. B., Olde Damink, L. H., Dijkstra, P. J., Feijen, J., & Nieuwenhuis, P. (1992). Secondary cytotoxicity of cross-linked dermal sheep collagens during repeated exposure to human fibroblasts. *Biomaterials*, *13*, 1017–1024.

Woessner, J., Jr. (1961). The determination of hydroxyproline in tissue and protein samples containing small proportions of this imino acid. *Archives of Biochemistry and Biophysics*, *93*, 440–447.

Wu, X., Ye, Y., Chen, Y., Ding, B., Cui, J., & Jiang, B. (2010). Selective oxidation and determination of the substitution pattern of hydroxypropyl guar gum. *Carbohydrate Polymers*, *80*, 1178–1182.

Zhao, X., Kim, J., Cezar, C. A., Huebsch, N., Lee, K., Bouhadir, K., et al. (2011). Active scaffolds for on-demand drug and cell delivery. *Proceedings of the National Academy of Sciences*, *108*, 67–72.